3D reconstruction and capsid protein characterization of grass carp reovirus

FANG Qin[1], Shah Sanket[2], LIANG Yuyao[2] & Z. H. ZHOU[2]

1. State Key Laboratory of Virology, Wuhan Institute of Virology, Chinese Academy of Sciences, Wuhan 430071, China;
2. Department of Pathology and Laboratory Medicine, University of Texas Medical School at Houston, Houston TX 77030, USA
Correspondence should be addressed to Fang Qin (email: qfang@wh.iov.cn) or Z. H. Zhou (email: z.h.zhou@uth.tmc.edu)

Received November 23, 2004; revised May 17, 2005

Abstract Grass carp reovirus (GCRV) is a relatively new virus first isolated in China and is a member of the *Aquareovirus* genus of the *Reoviridae* family. Recent report of genomic sequencing showed that GCRV shared high degree of homology with mammalian reovirus (MRV). As a step of our effort to understand the structural basis of GCRV pathogenesis, we determined the three-dimensional (3D) structure of GCRV capsid at 17 Å resolution by electron cryomicroscopy. Each GCRV capsid has a multilayered organization, consisting of an RNA core, an inner, middle and outer protein layer. The outer layer is made up of 200 trimers that are arranged on an incomplete *T*=13 icosahedral lattice. A characteristic feature of this layer is the depression resulting from the absence of trimers around the peripentonal positions, revealing the underlying trimers on the middle layer. There are 120 subunits in the inner layer arranged with *T*=1 symmetry. These structural features are common to other members of the *Reoviridae*. Moreover, SDS-PAGE analysis showed that GCRV virions contain seven structural proteins (VP1-VP7). These structural proteins have a high degree of sequence homology to MRV, consistent with the structural similarities observed in our study. The high structural similarities of isolated GCRV and MRV suggest that future structural studies focusing on GCRV entering into and replicating within its host cell are necessary in order to fully understand the structural basis of GCRV pathogenesis.

Keywords: grass carp reovirus (GCRV), electron cryomicroscopy, three-dimensional structure, capsid protein.

DOI: 10.1360/062004-105

Grass carp reovirus (GCRV) is the first aquatic virus isolated and characterized in mainland China[1]. In 1983, it was reported that GCRV was the agent that caused severe outbreaks of infectious hemorrhage disease in grass carp (*Cyenopharyngodon idellus*). Subsequently, a series of relatively systematic analyses have been conducted to characterize the biological and molecular properties of GCRV[2−8]. More than 50 aquareoviruses have been identified since the first reovirus-like virus was isolated from aquatic tissues by Meyers in 1979[9]. Many of these isolates cause asymptomatic infection or infections with very minor diseases. It has been recognized that GCRV is the most pathogenic among all aquareovirus isolates reported to date[10,11]. Therefore, GCRV provides a good model system to study aquareovirus replication and pathogenesis and such studies also have significance in the fish farming agriculture.

GCRV has been classified as a member of genus *Aquareovirus* of family *Reoviridea*. GCRV virion has a multilayered spherical structure enclosing a genome

consisting of 11 segments of dsRNA[3]. Due to the lack of standard serotypes, classification of aquareovirus into the *Aquareovirus* genus is currently done mainly based on RNA∶RNA hybridization[12]. According to Rangel et al.[10], six different genetic groups (*Aquareovirus* genogroups A—F) have been identified among aquareovirus isolates based on reciprocal RNA blot hybridization and those not belonging to genogroups A—F, such as GCRV, are classified into group G. More recently, genetic sequences and phylogenic analyses of GCRV and three other aquareovirus isolates have suggested that GCRV is a member of genogroup C[8]. Further sequences comparisons showed that GCRV has a common evolutionary origin with mammalian reovirus (MRV) with a high level of sequence homology. The three-dimensional (3D) structure of a striped bass reovirus (a member of the genogroup A) and its structural changes upon trypsin treatment have been reported, which showed structures similar to those of mammalian reovirus particles[13,14]. A preliminary 3D structure of GCRV at 35-Å resolution was first reported by Xu et al.[15], however, a detailed structural comparison with other reoviruses was not possible due to the low resolution of that 3D map.

Among the nine genera of the *Reoviridae*, substantial progress has been made in the structural and functional studies of members in the orthoreovirus, rotavirus, orbivirus, phytoreovirus, cypovirus genera[16—20]. In contrast, much less is known about the structural properties of aquareoviruses. As a step toward understanding the structural basis of GCRV pathogenesis, we determined the 3D structure of GCRV by electron cryomicroscopy (cryoEM) to 17-Å resolution and correlated with its biochemical and genetic analyses. Our results revealed detailed structural organization and protein subunit features of GCRV, thus laid a foundation for future studies aimed at understanding the structure function relationships during GCRV infection and replication.

1 Materials and methods

1.1 Cell and virus stain

CIK (*Ctenopharyngodon idellus* kidney) cell line, established by Zuo et al.[21], was used for the propagation of GCRV. Strain GCRV873 was isolated from Shaoyang, Hunan Province in China and stored in the author's laboratory[3].

1.2 Virus purification

GCRV capsids were pelleted from virus-containing cell culture media through a 30% sucrose cushion at 40000 rpm (250000 *g*) in a Sorvall rotor (SW41T1) for 2 h, 4℃. The resulting pellet was re-suspended in 10 mmol/L phosphate buffered salient (PBS) and loaded onto a 15%—50% sucrose gradient and centrifuged in a Sorvall SW41T1 rotor at 30000 rpm (120000 *g*) for 1 h, 4℃. A sharp band was clearly visible in the gradient and was collected and checked through negative stain transmission electron microscopy to confirm the presence of highly purified virus particles. SDS-polyacrylamide electrophoresis (SDS-PAGE) was used to reveal the protein components of the virus preparation[22]. This band was resuspended in 4 mL of PBS and pelletted by centrifugation at 40000 rpm (214000 *g*) in a Sorvall rotor (AH-650), 4℃ for 2 h. The pellet was resuspended in PBS to make a concentration of about 1 mg/mL for cryoEM sample preparation.

1.3 CryoEM

CryoEM of GCRV capsids was performed using established procedures. Briefly, 2.5 μL of purified sample was applied to carbon-coated Quantifoil holey grids with 2 μm-diameter holes (Quantifoil Micro Tools GmbH, Germany) and quickly frozen in liquid ethane so that the virions were suspended in a thin layer of vitreous ice across the holes of the supporting film. Digital cryoEM images were recorded at an effective magnification of 83062× and 200 kV in a JEOL 2010F FEG transmission electron cryomicroscope, which is equipped with a Gatan 4k × 4k CCD digital camera (Gatan, Pleasanton Ca.). Focal pair CCD pictures of 4k × 4k size were recorded and preprocessed for translation and rotation correction using the JAMES semi-automatic data collection program[23]. An electron dose of ~12 electrons·Å^{-2}·micrograph^{-1} was used. The electron beam was underfocused with a 1.8 μm difference between close-to-focus (~1 μm un-

der-focus) and far-from-focus (~2.8 μm under-focus) pictures in each focal pair. The pixel size of the CCD images is equivalent to 1.805 Å/pixel at the specimen level. For data processing, all images were averaged by combining adjacent pixels to yield a final sampling size of 3.61 Å/pixel at the specimen scale.

1.4 Data processing and 3D reconstruction

Imaging processing and 3D reconstruction was performed with our established procedure using the IMIRS software package[24,25] in a Microsoft Windows XP PC. Focal pair method was used for orientation estimation[25]. Briefly, individual GCRV particles were boxed out from far-from-focus digital images. A list of initial orientation estimates were first generated for each particle image using common-lines[26]. A preliminary model was then computed from 20 particles that showed the best self-common-line phase residuals and that had been refined by cross-common-line phase residual minimization among all 20 particles. The incorrect orientations were then eliminated from the list of initial orientation estimates of each particle by evaluating the cross-common-line phase residual between the particle and projection images of the preliminary model. The selected orientations were then refined by a global refinement which minimized the cross-common-line phase residuals across all selected particles and later with a projection-based refinement that optimized the match between the image and the projections computed from the initial 3D model. The new model reconstructed from these refinements was used as a template for the next round of particle selection and refinement, resulting in a further improved model. This process was iterated several times until no further improvement in the cross-common-line phase residual between particle images and the computed projections were noted. The orientations of the far-from-focus particle images were directly used as the starting orientations for their corresponding close-to-focus particles and were further refined iteratively as described above. The final structure was computed to 17 Å-resolution by merging 348 particles extracted. The 3-D visualization of the generated structure was carried out using Iris Explorer (NAG, Inc., Downers Grove, Ill.).

2 Results and discussion

2.1 GCRV purification

A large quantity of purified GCRV particles was obtained by using density gradient centrifugation method. A transmission electron micrograph (TEM) image of negatively stained preparation is presented in Fig. 1. The density gradient-purified GCRV particles appeared to have the same size and morphology with a clear double capsid shell structure organization.

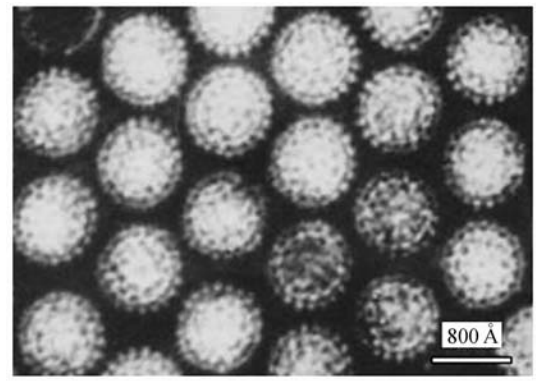

Fig. 1. Purified GCRV particles observed by TEM.

2.2 CryoEM image of GCRV

The close-to-focus and far-from-focus cryoEM images of a representative focal pair of GCRV embedded in vitreous ice is shown in Fig. 2(a) and (b), respectively. The GCRV virion was rather spherical with no recognizable surface spikes. Fig. 2(c) and (d) also show the corresponding power spectrum computed from the close-to-focus and far-from-focus images shown in Fig. 2(a) and (b), which showed that there was high-resolution information stored in these images. It was evident from these spectra that the furthest ring of contrast transfer function (CTF) in the spectrum of the far-from-focus extended out to 1/15 $Å^{-1}$ while that in the close-to-focus reached 1/9$Å^{-1}$.

2.3 Radial density plots

The radial density distribution of the GCRV particle reconstruction is shown in Fig. 3. This plot shows the distribution of the virion particle densities as a function of radius. Four distinctive sections can be resolved in each intact GCRV particle, corresponding to

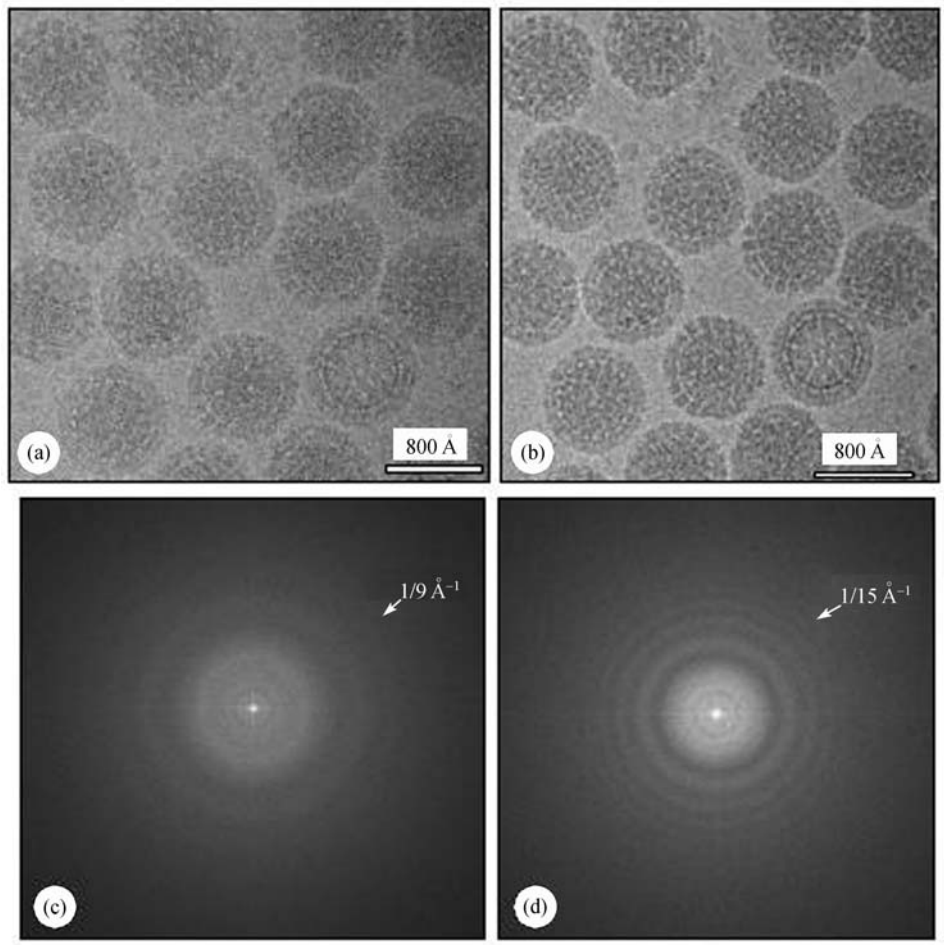

Fig. 2. A focal pair cryoEM pictures of GCRV and their power spectra. (a) and (b), Close-to-focus (a) and far-from-focus (b) cryoEM images; (c) and (d), power spectra of close-to-focus (c) and far-from-focus (d) images.

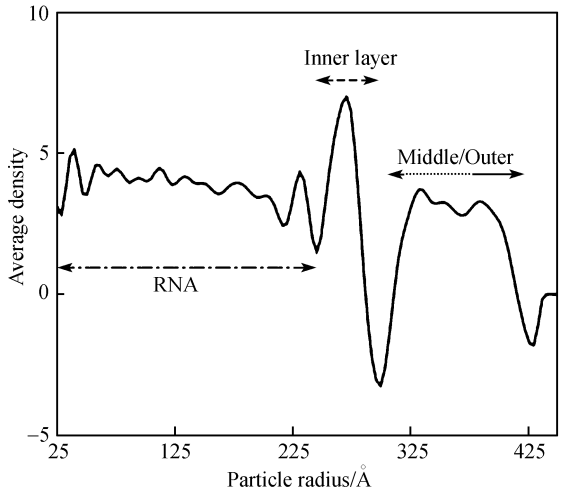

Fig. 3. GCRV radial density plots. Different dashed line denotes the RNA core, the inner, middle, and outer layers, respectively.

viral RNA core, inner layer, middle layer and outer layer. Their radii were 0—240 Å, 240—285 Å, 285—370 Å, 370—410 Å, respectively.

2.4 GCRV 3D reconstruction

The 17 Å reconstruction of GCRV was displayed using shaded surface representation color-coded according to particle radius and examined along an icosahedral three-fold from outside (Fig. 4(a)) and inside using cutaway view (Fig. 4(b)). Each GCRV particle has a diameter of 820 Å composed of multiple layers of densities. The outer layer consists of 600 subunits arranged on an incomplete T=13 icosahedral lattice and is ~40 Å in thickness. Surrounding each icosahedral 3-fold symmetry axis are 3 characteristic density

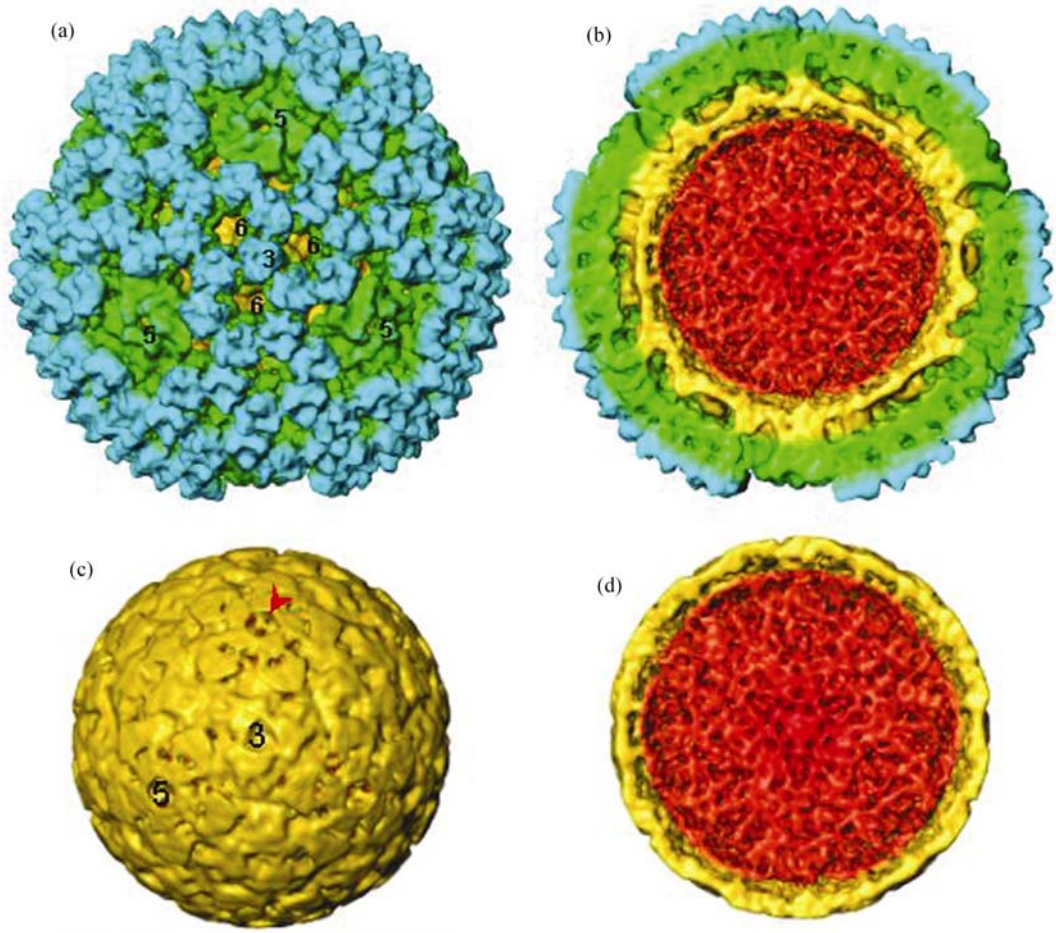

Fig. 4. 3D reconstruction of GCRV. (a) Shaded surface representations of GCRV reconstruction viewed along an icosahedral threefold axis. The 3D map is color coded according to particle radius such that RNA core is red, inner layer is orange, middle layer is green and the outer layer with 6-fold related trimeric subunits is aquamarine. “3”, “5”, and “6” represent icosahedral 3-, 5-, and local 6-fold axes. The surface view reveals that the outer layer is composed of 600 subunits arranged on an incomplete T=13 icosahedral lattice. The absence of trimers around each 5-fold axis results in depressions around the 5-fold axes that expose underlying subunit arrangement. (b) Cutaway view revealing different layers of density. (c) Shaded representation of inner layer as viewed along a 3-fold axis including densities up to a radius of 285 Å, revealing 60 dimers arranged on a T=1 icosahedral lattice. A channel penetrating the inner layer is observed at each 5-fold axis (red arrow). (d) Cutaway view of the inner layer and RNA core (red) as viewed along a 3-fold axis.

rings, each made up of 6 shared trimers related by local 6-fold axes (Fig. 4(a)). These intra- and inter-trimeric interactions led to the formation of a network of connected densities on the outer shell that provide further stabilization of the outer layer. A distinguishing feature on the outer layer was the 5-fold proximal depressions resulting from missing peripentonal trimers. The absence of these trimers exposes the protein subunit arrangement of the inner layer. This structure organization shares striking similarity to that of the MRV[16]. Interestingly, Rotavirus, which also contains a genome of 11 dsRNA segments, comprises 260 subunits of trimers on outer layer[17], thus having a different outer shell structure. Further careful structural comparison of GCRV and MRV indicates that they shared many similarities[27]. The only difference is that MRV contains a hemagglutinin protein σ1 for cell attachment which is located at the distal end of the 5-fold axis[16], but no such protein was identified in GCRV.

The characteristics of the inner layer include a channel along each 5-fold axis (Fig. 4(c)). The inner

layer has a diameter of about 570 Å and consists of 60 dimers arranged on a *T*=1 icosahedral lattice (Fig. 4(c)). Radial dissection of GCRV structure encompassing only the inner layer further showed that these channels transversed through the inner layer and connect to the RNA shell (Fig. 4(d)), which appeared to be common to other members of the *Reoviridae*, such as MRV, BTV, Rotavirus, suggesting a similar endogenous RNA replication mechanism within an intact virus particle may be employed by all these viruses[28]. Examination of the arrangement of the 200 trimers on the outer and middle layers and the 120 subunits on the inner core suggests that each subunit of the inner layer interacts with two subunits of the middle layer, thus strengthening the interlayer interactions. The core of the particle contains an RNA shell located underneath the inner layer (Fig. 4(d)). Moreover, the structural organization of two distinct shells encloses a highly ordered RNA layer, which may provide an optimal position and the necessary space for endogenous transcription and releasing into host cell. The inner layer might assist transcription, and the channels might facilitate exit of transcribed nascent RNA; whereas, the trimers of the outer layer might play a role in interaction with host cells[29].

2.5 Capsid protein analysis

To further identify the components of matured GCRV capsid, the purified virion was analyzed by using SDS-polyacrylamide (SDS-PAGE) gel (Fig. 5). Seven structural protein components were identified with molecular weight about 138, 137, 136, 79, 67, 43, 34 kD respectively. Three of the seven proteins VP1, VP2 and VP3 have similar, large molecular mass. VP6 and VP7 have small molecular mass. In addition, VP5 was the most abundant protein while VP4 was the least. These results were consistent with both aquareovirus and MRV protein properties[12,16], and prediction results deduced from genome amino acid sequences of GCRV[5,8].

Based on sequence analysis and homology between GCRV and MRV, we can predict that among the seven structural proteins in GCRV, five form the inner and middle layers, including VP1, VP2, VP3, VP4 and VP6, corresponding to λ2, λ3, λ1, μ2, σ2 in MRV, respectively. These proteins may play a role in virus transcription and replication. VP5 and VP7 were assigned as outer shell proteins, corresponding to μ1 and σ3 of MRV, having similar structural and function roles, which might be related to virus entry and interaction between virus and host cells during infection[16].

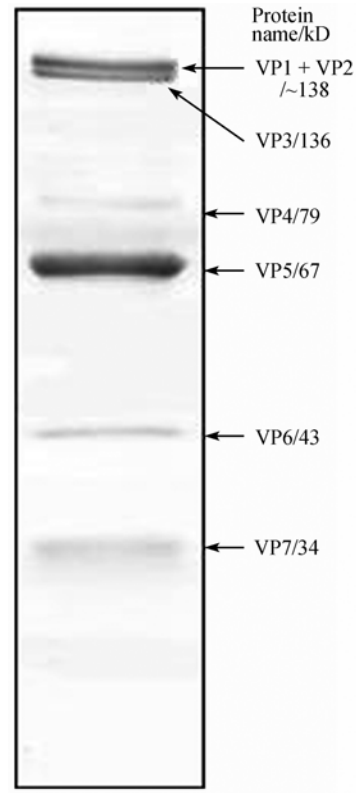

Fig. 5. SDS-PAGE analysis of GCRV virion protein.

GCRV VP3 was a primary component of in the inner layer. Because GCRV VP1 and MRV λ2 share similar enzymatic domains, we propose that VP1 is the turret protein that decorates the five-fold vertices. Indeed, GCRV VP1 contains two methylase domains and other domains responsible for nascent RNA processing and release[16]. VP2 was defined as particle-associated reovirus RNA polymerase (MRV analogue λ3), which is likely to be located inside the inner layer around each fivefold vertex to participate in initiation of syntheses of mRNA. VP4 (MRV analogue μ2) might be a coadjutant of VP2 for facilitating ini-

tiation and elongation of mRNA. VP6, similar to σ2 protein in MRV, might be a stabilizing clamp to enhance VP3 (λ1 analogue) core frame intensity[28]. It should be pointed out that in the non-turreted members of in family *Reoviridae*, such as in Orbiviruses and rotaviruses, there is no σ2-protein or its homolog, the proteins that constitute the innermost shell (VP2 and VP3 in rotaviruses and orbiviruses, respectively) can self-assemble into icosahedral particles[28].

In the outer layer, GCRV VP5 and VP7 were present in virions with 1∶1 ratio, corresponding to MRV μ1 and σ3, having similar structure and function. Our 3D model shows that these two proteins have the same copy number, i.e. 200 trimers. As revealed in Fig. 5, VP5 was also the most abundant protein in GCRV, similar to MRV μ1[16]. It might be located in the intermediate layer of the particle (see Fig. 4(a) and (b), green mark). The trimers on the outer shell might function as a receptor recognition site during virus and host cell interaction and entry of virus into host cells[16].

No fibre-like hemagglutinin structure was found in GCRV, which is same as another aquareovirus SBRV[13], different from MRV (σ1 protein). The purified virions maintained their intact structure as revealed by both TEM and cryo-EM, it is unlikely the fibre-like structure was lost or degraded during sample purification. Although the precise role of hemagglutination in reovirus infection is unknown, the absence of a hemagglutinin in GCRV suggests that the way of host cell to recognize GCRV might be different from that for MRV.

Previous study has showed that the genomic structure and sequences of GCRV and MRV shared the high level of identity[5,8]. This high level of identity is reflected in their structures[30]. The structure of GCRV reported here resembles that of the MRV. Several differences between GCRV and MRV indeed exist, such as numbers of genome segments, antigenicity, cytopathic effects and host spectrum, reflecting their divergent evolutiontrait. In this regard, determination of GCRV structure at high resolution and its conformation changes during virus transcription will help to elucidate the molecular and structural mechanism of its transcription regulation.

Acknowledgements We thank Dr. Yu Xuekui for technical help in virus purification, Mr. Ivo Atanasov for assistance in cryoEM, and Dr. Wah Chiu for providing access to the cryoEM facility at the National Center for Macromolecular Imaging supported by NIH (Grant No. P41RR02250). The research in Dr. Zhou's lab is supported by NIH (Grant Nos. AI46420 & CA94809), the Welch Foundation (AU-1492) and the American Heart Association (Grant No. 0240216N). This work was supported by the National Natural Science Foundation of China (Grant Nos. 30170730 & 30470074).

References

1. Chen, B. S., Jiang, Y., Morphological and physicochemical characterization of the hemorrhagic virus of grass carp, Kexue Tongbao, 1984, 29, 832－835.
2. Fang, Q., Ke, L.H., Cai, Y. Q., Growth characterization and high titer culture of GCHV, Virol. Sinica (in Chinese), 1989, 3: 315－319.
3. Ke, L. H., Fang, Q., Cai, Y. Q., Characteristics of a novel isolate of grass carp hemorrhage virus, Acta Hydrobiol. Sinica (in Chinese), 1990, 14: 153－159.
4. Huang, J., Ke, L. H., Cai, Y. Q., Reaction core of grass carp hemorrhage virus, Acta biochem. Biophys. Sinica (in Chinese), 1992, 24(2): 132－139.
5. Fang, Q., Attoui, H., Francois, J. et al., Sequence of genome segments 1, 2 and 3 of the grass carp reovirus (Genus Aquareovirus, Family Reoviridae), Biochem. Biophys. Res. Commun., 2000, 274(3): 762－766. [DOI]
6. Zou,G. P., Fang, Q., Study on replication and morphogenesis of the grass carp reovirus (GCRV) in CIK Cells, Virol. Sinica (in Chinese), 2000, 15(3): 188－192.
7. Fang, Q., Zhu, Z. Y., Expression of grass carp reovirus (GCRV) RNA dependent RNA polymerase (RdRp) gene function domain in E. Coli, J. Chin. Virol. (in Chinese), 2002, 18(1): 86－88.
8. Attoui, H., Fang, Q., Jaafar, F. M. et al., Common evolutionary origin of aquareoviruses and orthoreoviruses revealed by genome characterization of Golden shiner reovirus, grass carp reovirus, striped bass reovirus and golden ide reovirus (genus Aquareovirus, family Reoviridae), J. Gen. Virol, 2002, 83(8): 1941－1951.
9. Meyers, T, R., A Reo-like virus isolated from juvenile American oysters (Crassostrea virginica), J. Gen. Virol., 1979, 43: 203－212.
10. Rangel, A. A., Rockemann, D. D., Hetrick, F. M. et al., Identification of grass carp hemorrhage virus as a new genogroup of Aquareovirus, J. Gen. Virol., 1999, 80: 2399－2402.
11. Ahne, W., Viral infectious of aquatic animals with special reference to Asian aquaculture, Annual Review of Fish Diseases, 1994, 4: 375－388. [DOI]
12. Mertens, P. P. C., Arella, M., Attoui, H. et al., Family Reoviridae, in Virus Taxonomy. Seventh Report of the International Committee for the Taxonomy of Viruses, San Diego: Academic Press, 2000, 395－480.

13. Shaw, A. L., Siba, K., Samal, K. et al., The Structure of aquareovirus shows how the different geometries of the two layers of the capsid are reconciled to provide symmetrical interactions and stabilization, Structure, 1996, 4: 957－967.
14. Nason, E. L., Samal, S. K., Prasad, B. V. V., Trypsin-induced structural transformation in quareovirus, J. Virol., 2000, 74: 6546－6555. [DOI]
15. Xu, W., Zhang, X., Ke, L. H. et al., Cryo-electron microscope and 3 dimentional reconstruction of grass carp hemorrhage virus, Journal of Chinese Electron Microscopy Society (in Chinese), 1998, 17(4): 325－326.
16. Nibert, M. L., Schiff, L. A., Reoviruses and their replication, in Fields Virology (eds. Knipe, D. M., Howley, P. M.), Philadelphia: Lippincott Williams & Wilkins, 2001, 1679－1728.
17. Estes, M., Rotaviruses and their replication, in Fields Virology (eds. Knipe, D. M., Howley, P. M.), Philadelphia: Lippincott Williams & Wilkins, 2001, 1747－1785.
18. Grimes, J. M., Burroughs, J. N., Gouet, P. et al., The atomic structure of the bluetongue virus core, Nature, 1998, 395: 470－478.
19. Shao, C., Zhou, Z. H., Lu, G., The three-dimensional structure of the rice dwarf virus core, Science in China, Ser. C, 2001, 44(2): 192－198.
20. Zhou, Z. H., Zhang, H., Jakana, J. et al., Cytoplasmic polyhedrosis virus structure at 8 Å by electron cryomicroscopy: Structural basis of capsid stability and mRNA processing regulation, Structure, 2003, 11(6): 651－663. [DOI]
21. Zuo, W. G., Qian, H. X., Xue, Y. F. et al., Establishment of grass carp kidney cell line (CIK), Fresh-water Fisheries (in Chinese), 1984, (2): 38－39.
22. Sambrook, J., Fritsch, E. F., Maniatis, T., Molecular Cloning: A Laboratory Manual, 2nd ed., New York: Cold Spring Harbor, 1989.
23. Booth, C. R., Jiang, W., Baker, M. L. et al., A 9Å single particle reconstruction from CCD captured images of a 200 kV electron cryomicroscope, J. Struct. Biol., 2004, 147(2): 116－127. [DOI]
24. Liang, Y., Ke, E. Y., Zhou, Z. H., IMIRS: A high-resolution 3D reconstruction package integrated with a relational image database, J. Struct. Biol., 2002, 137: 292－304. [DOI]
25. Zhou, Z. H., Chiu, W., Determination of icosahedral virus structures by electron cryomicroscopy at subnanometer resolution, Adv. Protein Chem., 2003, 64: 93－124.
26. Crowther, R. A., Procedures for three-dimensional reconstruction of spherical viruses by Fourier synthesis from electron micrographs, Philos. Trans. R Soc. Lond. B Biol. Sci.,1971, 261: 221－230.
27. Nibert, M. L., Structure of Mammalian orthoreovirus particles, Curr. Top. Microbiol. Immunol., 1998, 233: 1－30.
28. Reinisch, K. M., Nibert, M. L., Harrison, S. C., Structure of the reovirus core at 3.6 Å resolution, Nature, 2000, 404: 960－967. [DOI]
29. Zhang, X., Walker, S. B., Chipman, P. R. et al., Reovirus polymerase lambda 3 localized by cryo-electron microscopy of virions at a resolution of 7.6 Å, Nat. Struct. Bio., 2003, 10: 1011－1018. [DOI]
30. Kim, J., Tao, Y., Karin, M. et al., Orthoreovirus and Aquareovirus core proteins: Conserved enzymatic surfaces, but not protein–protein interfaces, Virus Res., 2004, 101: 15－28. [DOI]